International Journal of Pharmaceutics 403 (2011) 15–22

Contents lists available at ScienceDirect

International Journal of Pharmaceutics

journal homepage: www.elsevier.com/locate/ijpharm

Confocal laser scanning microscopy (CLSM) based evidence for cell permeation by mono-4-(N-6-deoxy-6-amino-β-cyclodextrin)-7-nitrobenzofuran (NBD-β-CyD)

Hai Wei*, Weizhong Zheng[1], James Diakur[2], Leonard I. Wiebe[3]

Centre for Chinese Medical Therapy and System Biology, Shanghai University of Traditional Chinese Medicine, Shanghai, China

ARTICLE INFO

Article history:
Received 24 June 2010
Received in revised form 7 September 2010
Accepted 27 September 2010
Available online 7 October 2010

Keywords:
β-Cyclodextrin
NBD-adamantine
NBD-glucose
4-Chloro-7-nitrobenz-2-oxa-1,3-diazole (NBD)
Confocal laser scanning microscopy (CLSM)
Intracellular uptake in vitro

ABSTRACT

Beta-cyclodextrin (β-CyD), amantadine and glucose were fluorescently tagged with 4-chloro-7-nitrobenz-2-oxa-1,3-diazole (NBD chloride) to afford NBD-β-CyD, NBD-amantadine and NBD-glucose, respectively. NBD-β-CyD/amantadine and β-CyD/NBD-amantadine inclusion complexes were prepared. Fluorescence emission maxima (λ_{max} 544 nm) and relative fluorescence intensities for NBD-β-CyD and NBD-β-CyD/amantadine were virtually identical, precluding the use of emission spectrum shifts for distinguishing free NBD-β-CyD from the complex. Intracellular accumulation of NBD-β-CyD was studied in HepG2 and SK-MEL-24 cells using confocal laser scanning microscopy (CLSM). No major differences were observed between uptake of NBD-β-CyD and NBD-β-CyD/amantadine. Serum proteins did not perturb uptake, whereas temperature-dependent uptake, indicative of cell entry via diffusion, was observed. Intracellular distribution favoured mitochondria, with less fluorescent material present in cytoplasm and none in cell nuclei. No experimental evidence of NBD-β-CyD breakdown to NBD-glucose was found upon chromatographic analysis of incubation mixtures, providing additional evidence of intact NBD-β-CyD entry into these cells. Endocytosis and/or cholesterol-independent membrane modulation are discussed as possible mechanisms for the transmembrane passage of NBD-β-CyD.

1. Introduction

Cyclodextrins (CyDs) are cyclic α-(1,4)-linked oligosaccharides of α-D-glucopyranose. β-Cyclodextrin (β-CyD) comprises seven-glucose units and has near-ideal cavity dimensions (Φ = 6.2 Å) for complexing small drug molecules (Szejtli, 1988). CyDs are relatively large (MW = ~1000–>1500 Da), neutral molecules that are poor permeants of biological membranes (Matsubara et al., 1995; Masson et al., 1999). It is well established that CyDs disappear rapidly from the systemic circulation after intravenous (i.v.) dosing in animals, and that they are excreted mainly via the kidney (Kubota et al., 1996). CyDs facilitate their own absorption at high oral doses (Irie and Uekama, 1997), and nasal absorption in rats (Matsubara et al., 1995) is reported. Mechanisms by which CyDs promote passage of their guests across cell monolayers have been investigated (Marttin et al., 1999; Lambert et al., 1980, 2005) and guest transfer quantified (Matilainen et al., 2008) in cell culture. The successful delivery of the payload by these CyD complexes is clear, but it is not clear whether the CyD carrier itself crosses the membrane.

There are very few reports on the permeation of CyDs into cells, and the limited evidence for proof of cell permeation is largely inconclusive. ^{14}C-labelled β-CyD has been used to show oral absorption in rats (Szejtli et al., 1980) and to demonstrate that it extracts membrane components (cholesterol) from erythrocytes without entry of ^{14}C-labelled β-CyD into the erythrocyte (Gerloczy et al., 1985). CyDs can be transported into the cytoplasm of *Klebsiella oxytoca* (a bacterial pathogen) via a specific binding-protein dependent uptake system (Fiedler et al., 1996; Pajatsch et al., 1998). No analogous transport system has been identified in mammalian cells.

This manuscript describes the use of confocal laser scanning microscopy (CLSM) fluorescence imaging to observe and characterize cell permeation and sub-cellular distribution patterns of mono-4-(N-6-deoxy-6-amino-β-cyclodextrin)-7-nitrobenzofuran (NBD-β-CyD), a chemically substituted fluorescent β-CyD, under cell culture conditions. NBD-amantadine is a novel compound.

Abbreviations: CLSM, confocal laser scanning microscopy; NBD-β-CyD, mono-4-(N-6-deoxy-6-amino-β-cyclodextrin)-7-nitrobenzofuran.

* Corresponding author at: Centre for Chinese Medical Therapy and System Biology, Shanghai University of Traditional Chinese Medicine, 1200 Cailun Road, Pudong New District, Shanghai 201203, China. Tel.: +86 21 5132 2642; fax: +86 21 6810 2600.
E-mail address: wei_hai@hotmail.com (H. Wei).
[1] Current address: Labs-Mart Inc., 9411-20 Ave., Edmonton Research Park, Edmonton, AB, Canada T6N 1E5.
[2] Current address: Canam Bioresearch Inc., 6-1200 Waverley St., Winnipeg, MB, Canada, R3T 0P4.
[3] Current address: Department of Oncology, 1807 Cross Cancer Institute, 11560 Univ. Ave., Edmonton, AB, Canada, T6G 1N2.

0378-5173/$ – see front matter © 2010 Published by Elsevier B.V.
doi:10.1016/j.ijpharm.2010.09.032

2. Materials and method

2.1. Materials

Chemicals and materials were purchased from commercial suppliers: 4-chloro-7-nitrobenzofurazan (NBD-Cl) and adamantanamine hydrochloride (Lancaster Synthesis Ltd.), methyl α-D-glucopyranoside, β-cyclodextrin and sodium azide (Aldrich), preparative C18 bulk packing material (50–105 μm) (Waters), bovine plasma lipoprotein (Sigma). All chemicals were reagent grade and were used without further purification unless otherwise noted.

Fluorescence spectra were recorded using a SPEC FluoroMax® spectrofluorometer (SPEC Industries Inc., USA). A Labconco Freeze Dryer 3 was used for lyophilization. NMR spectra were recorded at 25 °C on either Bruker AM-300 or 500 MHz Varian VXR-500 NMR spectrometers. Chemical shifts are quoted in ppm, referenced to residual $CHCl_3$ at δ 7.27 for $CDCl_3$ solutions and HOD at δ 4.82 for D_2O solutions. Coupling constants (J) are reported in Hertz. ^{13}C NMR spectral assignments were aided by the J-MOD technique. The synthesized compounds were characterized by electrospray mass spectrometry (ES-MS) on a VG Trio-2000 quadrupole mass spectrometer (Fisons, UK). Thin-layer chromatography (TLC) was carried out on Kieselgel 60 F254 (Merck) with visualization under long-wavelength ultraviolet light or by charring with 5% methanolic sulfuric acid. Column chromatography was performed on silica gel 60 (230–400) Mesh ASTM, 0.040–0.063 mm (Rose Scientific Ltd.).

2.2. Confocal laser scanning microscopy (CLSM)

The confocal laser scanning microscope (Leica Microsystems Heidelberg GMBH, Germany) system included an argon–krypton laser with major emission lines of 488, 568 and 647 nm. Image analysis software (Leica Lasertechnik GmbH, Heidelberg) was run on a Motorola 68030 CPU workstation, using the OS-9 operating system. All physical parameters related to fluorescence illumination and detection were kept constant during the study: 512 × 512 pixel image, 100/1.32 oil-immersion objective lens, KP 510 short-pass excitation filter, TK 488 beam-splitter; the emission fluorescence was detected using a photomultiplier (gain 752 V), with a LP 515 barrier long-pass filter. Excitation and emission spectra of NBD-β-CyD and NBD-β-CyD/adamantidine were determined in aqueous solution (0.2 mg/mL).

2.3. NBD-G (**5**) was synthesized in four steps from methyl α-D-glucopyranoside using adapted literature methods

Methyl 6-azido-6-deoxy-α-D-glucoside (**2**) was recovered as a light hygroscopic yellow solid (11.6 g, 79%); mp 102–104 °C, lit. 103 °C (Hanessian et al., 1969); 6-azido-6-deoxy-D-glucose (**3**) was recrystallized from 2-propanol-ether to yield a white solid (1.23 g, 32%); mp 128–130 °C, lit. 128–133 °C (de Raadt and Stuetz, 1992). 6-Deoxy-D-aminoglucose hydrochloride (**4**) was recrystallized from a mixture of methanol–acetone to yield a white solid (0.35 g, 66%); mp 139–141 °C, lit. 158 °C (Hardegger et al., 1963). 6-Deoxy-N-(7-nitrobenz-2-oxa-1,3-diazol-4-yl)aminoglucose (NBD-G **5**) was purified by C18 reverse phase column chromatography using a gradient of methanol–water for elution. Evaporation of the appropriate eluate fraction yielded an orange-red solid (90 mg, 16%), mp >185 °C (dec.). ^1H NMR (DMSO-d_6, 300 MHz) δ 6.61 (d, $J_{1,2}$ = 2.66 Hz, 1H, H-1α), 6.34 (d, $J_{1,2}$ = 8.86 Hz, 1H, H-1β); ^{13}C NMR (DMSO-d_6, 75 MHz) δ 146, 145.9, 144.8, 144.2, 137.4, 137.2(C_6H_6), 96.9(C-1α), 92.3(C-1β), 76.4(C-3β), 74.7(C-3α), 73.9, 72.7, 72.5, 72.2(C-2α, 2β, 5α, 5β), 72.0(C-4β), 69.8(C-4α), 46.1(C-6β), 45.9(C-6α). ES-MS m/z (M+1) 343.1, calcd for $C_{12}H_{14}N_4O_8$ 343.27. TLC (SiO_2) R_f 0.19 (9:3:1 chloroform–methanol–ammonia water), lit R_f 0.44 water saturated butanol on silica gel plates (Speizer et al., 1985).

2.4. NBD-β-CyD (**9**) was synthesized in four steps starting with β-CyD (Scheme 1) using modified literature procedures

Mono-6-deoxy-6-(p-tolylsulfonyl)-β-cyclodextrin (**6**) was recrystallized from hot water to yield a white solid (1.5 g, 26%); mp >163 °C (dec.), lit. mp 163–168 °C (dec.) (Brady et al., 2000). Mono-6-deoxy-6-azido-β-cyclodextrin (**7**) was synthesized from **6** and purified via the peracetylated intermediate (Petter et al., 1990; Tekeo et al., 1989) to yield a white solid (5.3 g, 84%); mp >209 °C (dec.). The peracetylated intermediate (**8**) (369 mg; 46%) was a white solid: R_f 0.11 (3:2 hexane–acetone); ^1H NMR (300 MHz, $CDCl_3$) δ 5.30–5.08 (m, 7H), 5.07–4.90 (m, 7H), 4.78–4.65 (m, 7H), 4.55–4.40 (m, 7H), 4.25–3.94 (m, 14H), 3.74–3.54 (m, 7H), 2.10–1.90 (m, 60H, $COCH_3$).

Mono-6-deoxy-6-amino-β-cyclodextrin (**8**). Using an alternative to the literature procedure (Hamasaki et al., 1993), 7 (1.9 g, 1.64 mmol) was dissolved in MeOH–H_2O (325 mL; 1:2) and Pd/C (10%, 300 mg) was added. This mixture was subjected to hydrogen gas (30 psi) at room temperature for 72 h. After removal of the catalyst by filtration, the solution was evaporated in vacuo to yield compound **8** as a white solid (1.7 g, 91%); mp 236 °C (dec.); TLC (SiO_2) R_f 0.11 (8:2:2 isopropanol–water–ammonium hydroxide); ^1H NMR (500 MHz, D_2O) δ 5.18–5.10 (m, 7H, H1), 4.0 (t, 7H, H3), 3.98–3.88 (m, 31H, H6, H5), 3.7 (dd, 7H, H2), 3.62 (t, 6H, H4), 3.54 (t, 1H, H4), 3.30 (dd, 1H, H6), 3.06 (dd, 1H, H6); ^{13}C NMR (D_2O, 75 MHz) δ 104.3, 104.2, 104.0, 83.6, 83.4, 83.3, 75.7, 75.6, 75.5, 75.4, 74.7, 74.6, 74.5, 74.4, 74.3, 74.2, 74.1, 73.7, 62.8; ES-MS positive ionization mode, calcd m/z 1134.01, found m/z 1135.7.

Mono-4-(N-6-deoxy-6-amino-β-cyclodextrin)-7-nitrobenzofuran (NBD-β-CyD **9**) was synthesized using general literature CyD derivatization procedures modified for this synthesis (Ikeda et al., 2006). β-$CyDNH_2$ **9** (15 mg, 13.2 μmol), NBD–Cl (7.9 mg, 39.7 μmol) and $NaHCO_3$ (15 mg, 0.18 mmol) were dissolved in water–methanol (2:1; 1.5 mL). The reaction mixture was stirred in the dark at room temperature for 15 h. The solvents were removed in vacuo and the dark brown residue was purified by C18 reverse phase column chromatography using methanol–water a gradient for elution. The product **9** (8 mg) was obtained in 47% yield as a pale yellow solid. R_f 0.27 (7:2:2 isopopanol–water–ammonium hydroxide); ^1H NMR (500 MHz, D_2O) δ 8.5 (br s, 1H, aromatic), 6.6 (br s, 1H, NH), 5.26 (d, 1H, H1 CyD), 5.18 (d, 2H, H1 CyD), 5.17 (d, 2H, H1 CyD), 5.11 (br s, 1H, H1 CyD), 5.03 (br s, 1H, H1 CyD), 4.29–3.57 (m, 42H); ES-MS in positive ionization mode: calcd m/z 1297.10, found m/z 1298.6, calcd m/z 1297.10. Reported (Irie and Uekama, 1997): TLC (n-butanol:ethanol:water 5:4:3) R_f 0.51; ^1H NMR (D_2O, 500 MHz): δ 4.89–5.13 (m, 7H, H-1), 6.43 (br s, 1H, aromatic), 8.45 (d, 1H, aromatic); (d, 1H, aromatic), 8.19 (d, 1H, aromatic). MALDI-TOF MS: m/z 1320.9, calcd for $[M+Na]^+$, 1320.1.

2.5. NBD-amantadine [4-(1-N-adamantanamino)-7-nitrobenzofuran; 10] (Scheme 2)

1-Adamantanamine hydrochloride (94.3 mg, 0.50 mmol), 4-chloro-7-nitrobenzofurazan (NBD-Cl, 100 mg, 0.50 mmol) and potassium carbonate (200 mg, 1.45 mmol) were dissolved in methanol (3 mL), and the reaction mixture was stirred in the dark for 24 h. The methanol was then evaporated in vacuo and the residue was dissolved in chloroform (50 mL) and washed with water (50 mL, 3 times). The organic solution was evaporated, and the residue was purified by silica gel column chromatography using 6:1 hexane–acetone as eluent to give **10** (27 mg; 17%) as an orange solid after lyophilization. R_f 0.71 (1:1 hexane–ethyl acetate); ^1H NMR (500 MHz, $CDCl_3$) δ 8.4 (d, 1H, J_d = 8.8 Hz, aromatic), 6.4 (d,

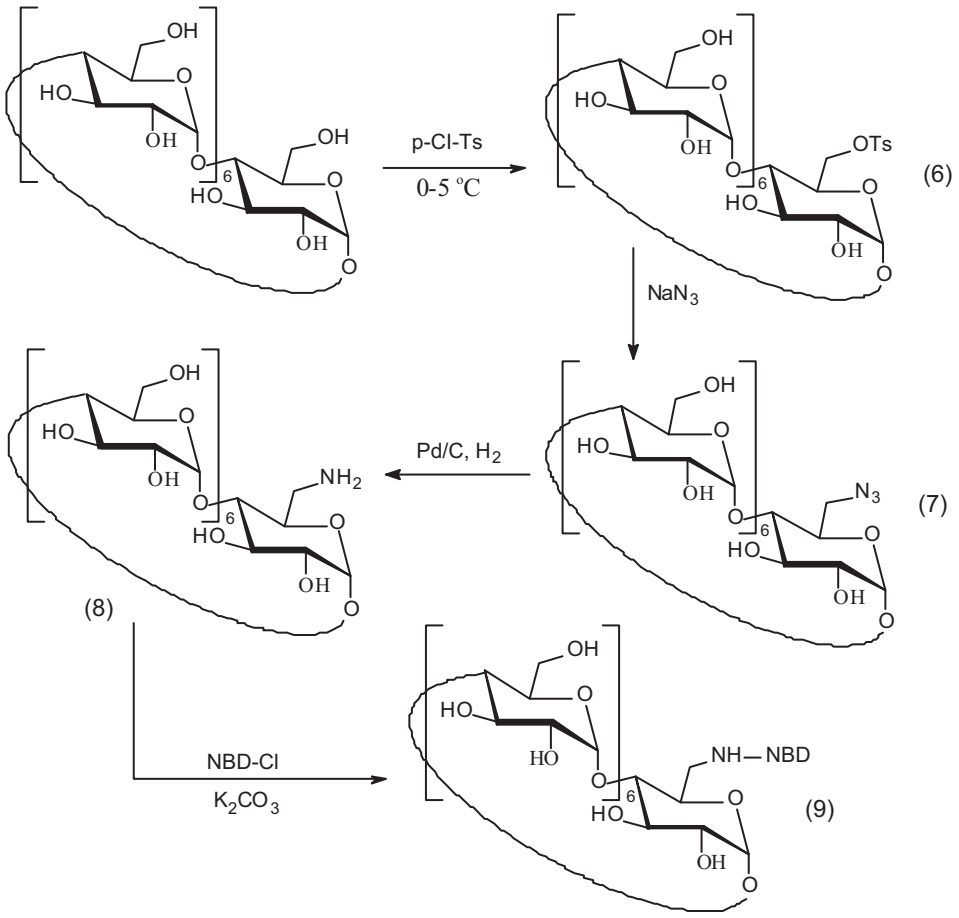

Scheme 1. Synthesis of mono-4-(N-6-deoxy-6-amino-β-cyclodextrin)-7-nitrobenzofuran (NBD-β-CyD, **9**).

1H, J_d = 8.8 Hz, aromatic), 6.15 (br s, 1H, NH), 2.2 (br s, 3H, adamantane γ-protons), 2.15 (br s, 6H, adamantane α-protons), 1.8 (m, 6H, adamantane β-protons).

2.6. NBD-β-CyD/amantadine inclusion complex

Amantadine (0.016 mmol) and NBD-β-CyD (0.016 mmol) were added to water (2 mL) and the mixture was mechanically stirred in the dark at 60 °C for 4 h, followed by lyophilization. Complexes were re-constituted in water and filtered (0.22 μm filter) immediately before use.

2.7. Stability of NBD-β-CyD in MEM and in RPMI-1640 cell culture media

NBD-β-CyD (1 mg/mL) was dissolved in each culture medium and incubated at 37 °C. Aliquots were withdrawn at 11 predetermined intervals (10–150 min) and examined by TLC, using 7:2:2 isopropanol–water–ammonium hydroxide as the solvent system. NBD-β-CyD and decomposition products (if any) were visualized on the TLC plate by long-wavelength light (for fluorescent compounds) and by charring with 5% methanolic sulfuric acid (for carbohydrates).

2.8. Intracellular uptake studies

HepG2 and SK-MEL-24 cells were maintained in MEM and RPMI-1640 medium, respectively. Both media contained 10% (v/v) fetal bovine serum (FBS) and 1% penicillin/streptomycin (v/v). The cells were grown in 75 mL flasks in an atmosphere of 5% CO_2 at 100% relative humidity, and passaged every 4 days. Two days prior to the uptake experiment, trypsinized HepG2 or SK-MEL-24 cells (2 mL) were plated into 3 cm petri dishes and grown as a monolayer

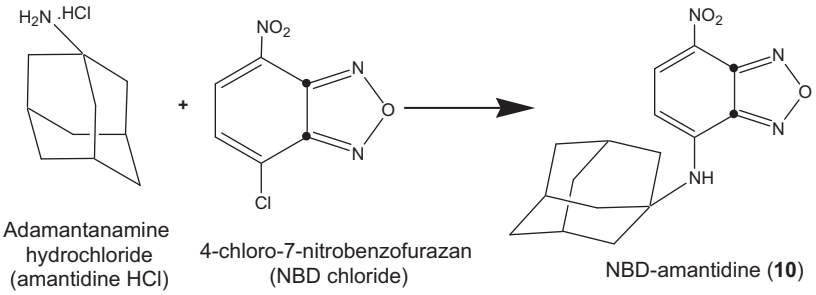

Scheme 2. Synthesis of fluorescently tagged amantadine (NBD-amantadine; **10**).

culture. The petri dishes containing the cells were rinsed gently with PBS (3×; pH 7.4), then test solutions of either NBD-β-CyD or NBD-β-CyD/amantadine (0.03 mg/mL in either MEM or RPMI-1640 for HepG2 or SK-MEL-24 cells, respectively) were added. These plates were incubated in the dark at specified temperatures for pre-determined times. After incubation, the medium was removed, and the monolayers were gently rinsed 3 times with PBS. A glass coverslip was directly mounted on the surface of the monolayer culture using a small amount of 1:1 PBS–glycerol. Control cultures were prepared identically. Three series of tests were carried out, to determine the effects of temperature (incubations at 0–2 °C or 37 °C for 30 min) and serum protein (with or without 10% FBS at 37 °C for 30 min), and to measure uptake-kinetics (with FBS or with 0.1%, w/v lipoprotein) at 37 °C over periods of 0.5, 2, 5, 15, 30 and 60 min.

2.9. Statistical analysis

Experiments were performed in triplicate. A minimum of three randomly chosen image regions of interest were selected for CLSM from each petri dish. For cytoplasm, over fifteen measurements were obtained from the images while for mitochondria, twenty to thirty measurements were obtained. The fluorescence images were stored on an optical disk for further analysis of fluorescence intensity within regions Quantitative intracellular uptake data were analyzed with SigmaPlot (v. 3.0). Significance of differences between experiments was calculated by Student's *t* test using two-tailed distributions and either a two-sample equal variance (homoscedastic) or a two-sample unequal variance (heteroscedastic) method. Statistical significance was calculated at the 95% confidence level ($p < 0.05$).

3. Results and discussions

3.1. Fluorescent probes

6-Deoxy-N-(7-nitrobenz-2-oxa-1,3-diazol-4-yl)aminoglucose (NBD-G; **5**) and 4-(N-Mono-6-deoxy-6-amino-β-cyclodextrin)-7-nitrobenzo-furan (NBD-β-CyD, **9**), were synthesized using established carbohydrate chemistry methods. Both are known compounds (Speizer et al., 1985; Ikeda et al., 2006), respectively, but modified syntheses and additional NMR data are reported. The resonance at 6.6 (br s, 1H) has now been assigned to NH as a slow exchanging proton, since the original assignment at 6.43 (br s, 1H, aromatic) (Matsubara et al., 1995) is incompatible with the number of aromatic protons (two) actually present in the molecule. 4-(1-N-Adamantanamino)-7-nitrobenzofuran (NBD-amantadine, **10**) has been used as a fluorophore for chromatographic analyses of adamantanamine analogues (Higashi et al., 2006), but since chemical characterization was not previously reported, additional data are now presented. Amantadine was readily complexed with NBD-β-CyD, but NBD-amantadine formed water-insoluble complexes with β-CyD. In water, the fluorescence spectra of NBD-β-CyD and its amantadine complex had qualitatively and quantitatively similar emission maxima (544 nm), but exhibited qualitatively distinct excitation bands between 300 nm and 420 nm (Fig. 1). The fluorescence emission intensities (counts per second; cps) for the 407 nm excitation band were identical for NBD-β-CyD and NBD-β-CyD/amantadine ($3.46 \pm 0.06 \times 10^6$ and $3.44 \pm 0.08 \times 10^6$ cps, respectively (means ± SEM, $n = 3$; $p > 0.05$).

After incubation (1 h) of **9** in either MEM or RPMI-1640 culture medium, only one fluorescent spot, which could also be charred by 5% methanolic sulfuric acid and corresponded to pure NBD-β-CyD, was visible on TLC ($R_f = 0.27$). In aliquots withdrawn after the first hour, a faint second fluorescent spot ($R_f = 0.94$) that did not char was observed. The fluorescence intensity of this second spot

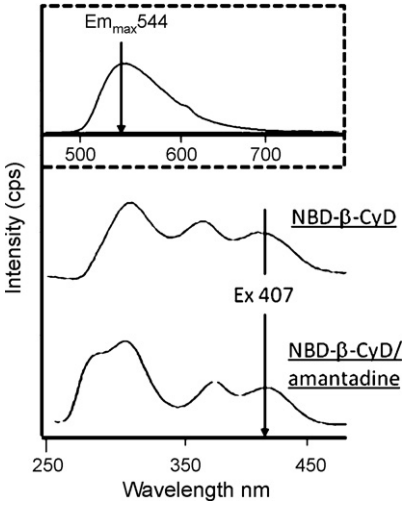

Fig. 1. Fluorescence excitation and emission spectra of NBD-β-CyD and NBD-β-CyD/adamantine in water (0.2 mg/mL). Fluorescence emission spectra (top), determined at an excitation (Ex) wavelength of 407 nm, were identical (Em_{max} 544 nm) for NBD-β-CyD and NBD-β-CyD/adamantine. Excitation spectra for NBD-β-CyD and NBD-β-CyD/adamantine are shown in the lower two spectra, as labeled. Fluorescence intensities are plotted as counts per second (cps).

increased with increasing incubation times, and after 2 h, a third spot ($R_f \approx 0.2$), not fluorescent, was visible after charring (β-CyD residue). At 150 min, the intensity of the third spot after charring was estimated to be ~25% of the intensity of the NBD-β-CyD spot in the same aliquot (i.e., ~25% decomposition after 2.5 h).

3.2. Intracellular uptake of NBD-β-CyD (*9*)

Typical fluorescence images of intracellular distributions of NBD-β-CyD are shown in Fig. 2. There were no qualitative differences in sub-cellular distributions of fluorescence between NBD-β-CyD and NBD-β-CyD/amantadine, and the subcellular distributions of both agents were similar in the two cell lines.

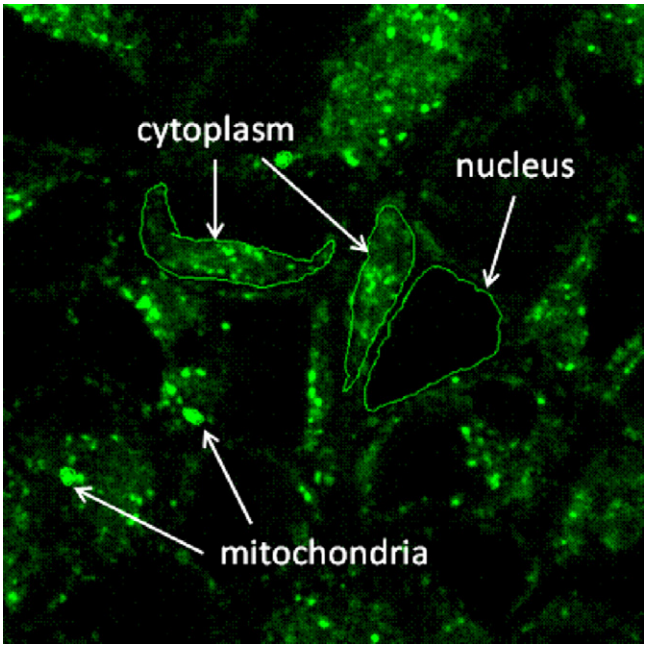

Fig. 2. CMSL image of SK-MEL-24 cells incubated with NBD-β-CyD **9** for 30 min in RPMI-1640 medium. Typical regions of interest elected for fluorescence assay are delineated by hand-drawn perimeters; cellular organelles are identified.

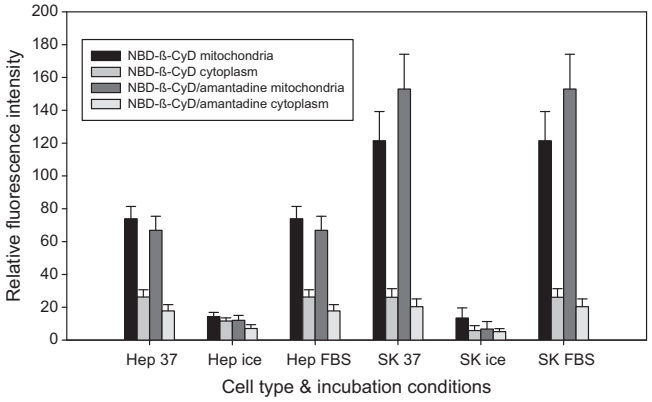

Fig. 3. Effects of temperature and protein on the intracellular uptake of NBD-β-CyD and NBD-β-CyD/amantadine by HepG2 and SK-MEL-24 cells in vitro. Error bars are standard deviations, for $n = 3$.

NBD-β-CyD fluorescence was not seen in nuclei. The cytoplasm was diffusely and granularly stained, and fluorescence was most intense in mitochondria, seen as bright green, oval and round foci distributed throughout the cytoplasm. Hand-drawn regions of interest selected for quantitation by fluorescence intensity integration are depicted in Fig. 2.

Temperature-dependent uptake was observed for both NBD-β-CyD and NBD-β-CyD/amantadine when incubated with either cell line at 37 °C or near 0 °C for 30 min in medium containing FBS (Fig. 3). The intracellular distribution patterns of NBD-β-CyD at the two different temperatures were similar (fluorescence mainly in the cytoplasm and mitochondria), but the fluorescence intensities were clearly temperature-dependent and significantly ($p < 0.01$) higher at 37 °C than 0 °C. Intensities (rfu) for **9** with HepG2 cells were 4.2 times (mitochondria) and 1.3 times (cytoplasm) higher at 37 °C, and 4.6 and 1.5 times higher for NBD-β-CyD-amantadine; with SK-MEL-24 cells, the intensities for mitochondria and cytoplasm with NBD-β-CyD **9** were 8.0 and 3.5 times higher at 37 °C, respectively, and for NBD-β-CyD-amantadine, 21.8 and 3.0 times higher, respectively.

The intracellular distribution of NBD-β-CyD was virtually independent of the presence or absence of FBS in the culture media, with fluorescence appearing in the mitochondria and cytoplasm (Fig. 3). Analysis (*t*-test) showed that the average fluorescence intensities for mitochondria and cytoplasm with NBD-β-CyD are significantly different ($p < 0.01$) for FBS vs. non-FBS in both cell lines. For NBD-β-CyD/amantadine, the fluorescence intensities in cytoplasm in SK-MEL-24 cells were significantly different ($p < 0.01$) for FBS vs. non-FBS. The average fluorescence intensities in mitochondria in both cell lines showed no significant difference between for FBS vs. non-FBS.

The intracellular uptake kinetics of NBD-β-CyD and NBD-β-CyD/amantadine complex in HepG2 and SK-MEL-24 cell lines were studied by repeated integration of the fluorescence intensity of selected regions over time. Representative uptake profiles for mitochondria and cytoplasm (Figs. 4 and 5) feature rapid initial (0–5 min) uptake followed by slower, linear increases between 5 and 60 min. Data for SK-MEL-24 cells were similar (not shown).

CLSM is a semiquantitative imaging technique that can be used to study intracellular uptake kinetics, subcellular distribution patterns, and permeation routes of fluorescent compounds across cell layers in vitro, without physical damage to the cell. Its major advantages over conventional fluorescence microscopy include the reduction of out-of-focus fluorescence, the ability to select clearly resolved optical sections of the tissue and extremely high sensitivity (Marttin et al., 1997; Skoog et al., 1998; Miller et al., 1997). Fluorescent detection and quantification of amantadine and CyDs,

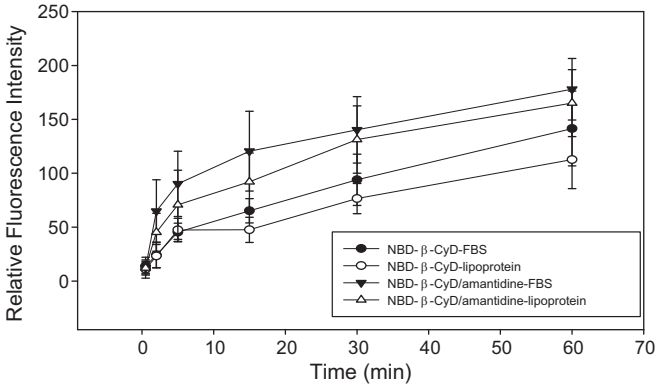

Fig. 4. Uptake kinetics of NBD-β-CyD and NBD-β-CyD/amantadine in the presence of added FBS or lipoprotein, in HepG2 mitochondria. Calculated regression equations: NBD-β-CyD & FBS ($Y = 1.74x + 38.67$; R^2 0.9969); NBD-β-CyD & lipoprotein ($Y = 1.27x + 36.10$; R^2 0.9695); NBD-β-CyD/amantadine & FBS ($Y = 1.51x + 90.81$; R^2 0.9641); NBD-β-CyD/amantadine & lipoprotein ($Y = 1.71x + 67.75$; 0.9969; R^2 0.9602).

requires derivatization because they fluorescence chromophores. 4-Chloro-7-nitrobenzofurazan (NBD-Cl), a fluorescence derivatization reagent for facile labelling of amines (Ghosh and Whitehouse, 1968) was selected for this work in conjunction with confocal laser scanning microscopy (CLSM) because of the impact NBD, a relatively low molecular weight fluorophore, is anticipated to impart on the processes to be measured.

The initial objective, to utilize complexes comprising non-fluorescent host/fluorescent guest (β-CyD/NBD-amantadine) and fluorescent host/non-fluorescent guest (NBD-β-CyD/amantadine) combinations, however could not be realized. Although NBD-β-CyD **9** and NBD-amantadine **10** were readily prepared, complexation of **10** with β-CyD produced a low water solubility product that was unsuitable for the purposes of this work. Attempts to produce more water-soluble complexes by introducing a linking arm (glycine) between adamantamine and NBD, or using an alternative (rhodamine) fluorescent label, yielded unstable adamantamine derivatives (data not shown), thereby negating this approach. These observations are in line with reports of formation of an insoluble complex between β-CyD and a nucleoside-derivatized amantadine (Yang et al., 2009).

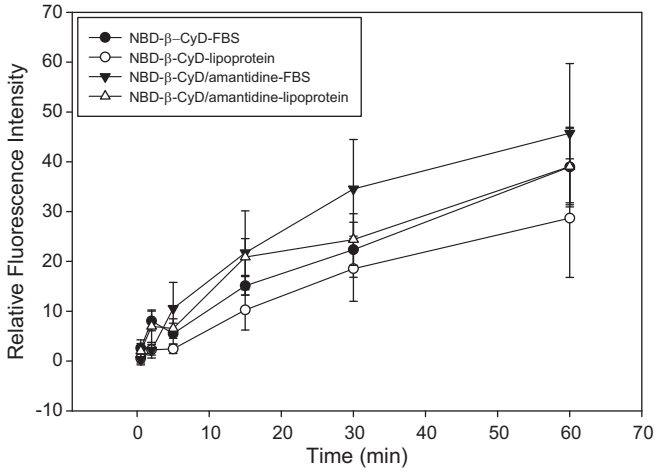

Fig. 5. Uptake kinetics of NBD-β-CyD and NBD-β-CyD/amantadine in the presence of added FBS or lipoprotein, in HepG2 cytoplasm. Calculated regression equations: NBD-β-CyD & FBS ($Y = 0.58x + 4.39$; R^2 0.9874); NBD-β-CyD & lipoprotein ($Y = 0.46x + 2.30$; R^2 0.9652); NBD-β-CyD/amantadine & FBS ($Y = 0.62x + 11.18$; R^2 0.9361); NBD-β-CyD/amantadine & lipoprotein ($Y = 0.53x + 8.02$; R^2 0.9214).

Uptake studies were consequently conducted using the fluorescent host NBD-β-CyD **9** and NBD-β-CyD/amantadine, the latter to minimize effect of cholesterol extraction by NBD-β-CyD as a permeation-perturbing effect (Yang et al., 2009). The quantification of fluorescence using CLSM necessitated determination of the effect of NBD-β-CyD/amantadine complex formation on the fluorescence spectra and yield. In the current work, no significant differences in fluorescent intensity or emission spectra were observed between NBD-β-CyD and NBD-β-CyD/amantadine, and excitation spectra exhibited only small differences, in agreement with literature data (Ikeda et al., 2006). This may be attributed to direct coupling of NBD to β-CyD (i.e., no spacer arm), which may sterically preclude intramolecular complexation. The high stability of β-CyD/adamantine and the similarities in fluorescence spectra and intensity of NBD-β-CyD and NBD-β-CyD/amantadine support the conclusion that formation of intramolecular and intermolecular complexes are unlikely to perturb their relative quantification using CMSL. However, this also negates the use of CMSL to obtain information on whether or not NBD-β-CyD is complexed once inside the cytoplasm or mitochondria.

Knowledge of the chemical stability of NBD-β-CyD is vital to interpretation of cell-associated fluorescence. CyDs are stable in alkaline medium, but are hydrolyzed to a series of linear maltosaccharides by strong acids. This ring-opening hydrolysis occurs at a much slower rate than the hydrolysis of linear oligosaccharides (Miyazawa et al., 1995). CyDs are less susceptible to attack by enzymes such as α-amylase and their enzymatic hydrolysis is slowed down even further when substituents are introduced on the hydroxyl groups (Irie and Uekama, 1997; Hirayama et al., 1992). None-the-less, NBD-G (NBD-glucose) is a possible CyD-ring hydrolysis product of NBD-β-CyD. However, TLC data indicate that NBD-β-CyD is stable under incubation conditions. Thus, evidence for the release of NBD- and β-CyD- residues, but not fluorescent carbohydrate fragments, precluded the further use of NBD-G in this work.HepG2 human hepatocellular carcinoma (Knowles et al., 1980) and SK-MEL-24 human melanoma (Guldberg et al., 1997) cells, were selected as representative human cancer cells that are used extensively in biochemical and drug-related cell studies. Incubation of either cell line with NBD-β-CyD or NBD-β-CyD/amantadine resulted in mitochondrial fluorescence intensities that were 3–4 times higher than that of comparable areas of cytoplasm devoid of mitochondria. Mitochondrial electron transport-linked oxidation is known to create an electrochemical proton gradient across the mitochondrial membrane, allowing positively charged molecules to distribute electrophoretically into the mitochondrial matrix based on the high negative transmembrane potential of mitochondria (Johnson et al., 1980; Grouselle et al., 1990). In the case of NBD-β-CyD, its secondary amine group would be expected to protonate, thereby creating a positive charge. This process could, at least in part, rationalize the movement of NBD-β-CyD, NBD-β-CyD/amantadine and other NBD-β-CyD complexes from the cytoplasm to the mitochondria.

It is possible to determine whether the intracellular uptake occurs via a specific receptor by studying the influence of temperature on intracellular uptake (Ostlund et al., 1996). Cooling is a practical way of lowering a cell's metabolism to demonstrate the mechanism of passive diffusion into cells. Energy-dependent processes such as active transport cannot occur near 0 °C (ice bath) because the carrier proteins that are responsible for active transport are tightly coupled to a source of metabolic energy, such as adenosine triphosphate (ATP) (Larsen et al., 1988). The observed temperature-dependent intracellular uptake of NBD-β-CyD is strongly supportive of a transmembrane permeation mechanism that is independent of a specific transport carrier. This clearly differentiates uptake into mammalian cells from bacterial uptake, as in the case of *K. oxytoca*, in which CyDs are internalized via a system of binding proteins specific for CyD transport (Feederle et al., 1996).

CyDs and their guests are in equilibrium in solution, so other components of the culture medium, especially albumin, cholesterol and lipoproteins, could possibly form complexes with NBD-β-CyD before, during or after transmembrane passage. However, in the current experiments, serum proteins only marginally influenced uptake into mitochondria and cytoplasm. This indicates that protein (including albumin and lipoprotein) complexation with NBD-β-CyD and NBD-β-CyD/amantadine was either minimal, and/or that it had no impact on the mechanism of absorption. This observation, combined with the very similar total cell accumulations of NBD-β-CyD and NBD-β-CyD/amantadine, would support an permeation mechanism that is largely independent of the CyD's ability to strip cholesterol from the cell membrane as a condition for entry into the cell. Published modeling studies have shown that adamantanes, with skeletal diameters of ∼5.15 Å, are a perfect fit for the β-CyD cavity (6.2 Å) (Eftink et al., 1989), in line with the high association constants of 10^5 M^{-1} characteristic of these complexes (Yang et al., 2009; Higuchi and Connors, 1965). The high stability of the β-CyD/amantadine complex was exploited in the current studies to elicit the role of membrane cholesterol stripping (by CyD) in modulating the membrane's impermeability to CyDs.

Kinetic uptake experiments were performed in two different media, one containing FBS and the other containing lipoprotein alone. The lipoprotein (90.8% HDL, 8.1% LDL) used in the experiments was obtained from bovine plasma. HDLs are physiological cholesterol acceptors that can induce the efflux of cholesterol from cells (Kilsdonk et al., 1995) and may affect the intracellular uptake of NBD-β-CyD and NBD-β-CyD/amantadine. Efflux of cholesterol would be the anticipated outcome when cells are in a medium containing a high concentration of HDL (0.1%, w/v). Intracellular uptake tests for the same preparations (NBD-β-CyD or NBD-β-CyD/amantadine) in both media were performed on the same day using the cells from the same source. Selected uptake profiles (Fig. 4) show that fluorescence increased rapidly in mitochondria within the first 5 min, then gradually increased during the next 45 min, whereas cytoplasmic fluorescence increased gradually over the entire period (Fig. 5); similar trends were apparent from other experiments (data not shown). Due to the high standard deviation for each time point, especially for mitochondria in both cell lines, it is not possible to conclude that there are differences between medium containing lipoproteins alone or containing FBS. The lack of distinct differences may be attributed to functional changes in the cell membrane due to HDL-induced cholesterol efflux or decreasing uptake of both NBD-β-CyD or NBD-β-CyD/amantadine lipoprotein complexation and precipitation.

It is known that CyDs can form inclusion complexes with lipids and extract cholesterol from biological membranes (Borroni et al., 2007), and that they stimulate efflux of cholesterol from cultured cells with high efficiency (Neufeld et al., 1996; Atger et al., 1997). Extraction of cholesterol changes the membrane's fluidity and permeability, and it has been postulated that these changes enable drug passage across the biological membrane (Masson et al., 1999).

There is a substantial body of evidence that depicts mammalian absorption of β-CyD and excretion of both metabolic fractions and the intact cyclodextrin (Kubota et al., 1996; Szejtli et al., 1980; Anderson et al., 1963). Kubota et al. (1996) concluded that only an insignificant amount of intact β-CyD was absorbed from the gastrointestinal tract in rats. Studies on healthy volunteers and ileostomy patients have shown that β-CyD and glucosyl-β-CyD were poorly digested in the human small intestine but they were readily fermented by the colonic flora, but that most of the administered CyD is excreted in the feces in the intact form (Flourie et al., 1993). Experimental evidence supports a model in which CyDs modulate the leakiness for some substrates through complex

processes initiated by extraction of cholesterol at tight junctions between epithelial cells (Lambert et al., 1980, 2005; Marttin et al., 1997; Hovgaard and Bronsted, 1995; Rodal et al., 1999), but these data are derived from cell monolayers, and do not model for the transmembrane model used in the present work.

The cell membrane is a highly selective filter that is impermeable to most polar molecules, and hydrophilic molecules cross cell membranes with difficulty unless they are substrates for transport by specialized transmembrane proteins or endocytosis. NBD-β-CyD is a moderately large, hydrophilic, secondary amine that is weakly protonated at physiological pH, and is expected to have low solubility in cell membranes. Diffusion-based membrane permeation would be expected to be negligible in these circumstances unless specialized conditions such as membrane disruption or endocytosis were to pertain. Endocytosis may be triggered by a number of mechanisms, and may be promoted by cholesterol sequestration. It can be rationalized that once inside the cell, diffusion into mitochondria would be followed by protonation and ionic trapping, at the expense of cytoplasmic NBD-β-CyD.

4. Conclusions

NBD-β-CyD, NBD-G and NBD-adamantine were synthesized as tracers for this study of cyclodextrin permeation into mammalian cells. The excitation and emission spectra, and the fluorescence yields of NBD-β-CyD and NBD-β-CyD/amantadine were found to be virtually identical and therefore appropriate for the semi-quantitative CLSM measurements used in the cell culture experiments. There was no evidence for the formation of NBD-G, a putative metabolic/chemical degradation product of NBD-β-CyD, under incubation conditions.

Extensive intracellular fluorescence after incubation of HepG2 and SK-MEL-24 cells with either NBD-β-CyD or NBD-β-CyD/amantadine was observed by CLSM. Intracellular fluorescence, putatively from NBD-β-CyD, was observed in mitochondria and cytoplasm, but not in cell nuclei. The intracellular uptake of NBD-β-CyD and NBD-β-CyD/amantadine was temperature-dependent, whereas serum proteins had no measurable effect on intracellular uptake of either substrate. These data are compatible with a transmembrane permeation mechanism that is independent of cholesterol stripping from the cell membrane by NBD-β-CyD or by high density lipoproteins. It is therefore postulated that NBD-β-CyD enters cells either via endocytosis or via an unspecified transmembrane diffusion process.

Acknowledgement

This work was supported in part through a grant from the Canadian Institutes for Health Research.

References

Anderson, G.H., Robbins, F.M., Domingues, F.J., Moores, R.G., Long, C.L., 1963. The utilization of scharfinger dextrins by the rat. Toxicol. Appl. Pharmacol. 5, 257.

Atger, V.M., Moya, M., Stoudt, G.W., Rodrigueza, W.V., Phillips, M.C., Rothblat, G.H., 1997. Cyclodextrins as catalysts for the removal of cholesterol from macrophage foam cells. J. Clin. Invest. 99, 773–780.

Borroni, V., Baier, C.J., Lang, T., Bonini, I., White, M.M., Garbus, I., Barrantes, F.J., 2007. Cholesterol depletion activates rapid internalization of submicron-sized acetylcholine receptor domains at the cell membrane. Mol. Membr. Biol. 24, 1–15.

Brady, B., Lynam, N., O'Sullivan, T., Ahern, C., Darcy, R., 2000. 6-O-p-Toluenesulfonyl-β-cyclodextrin. Org. Syntheses 77, 220.

de Raadt, A., Stuetz, A.E., 1992. A simple convergent synthesis of the mannosidase inhibitor 1-deoxymannonojirimycin from sucrose. Tetrahedron Lett. 33, 189–192.

Eftink, M.R., Andy, M.L., Bystrom, K., Perlmutter, H.D., Kristol, D.S., 1989. Cyclodextrin inclusion complexes: studies of the variation in the size of acyclic guests. J. Am. Chem. Soc. 111, 6765–6772.

Feederle, R., Pajatsch, M., Kremmer, E., Bock, A., 1996. Metabolism of cyclodextrins by *Klebsiella oxytoca* M5a1: purification and characterization of a cytoplasmically located cyclodextrinase. Arch. Microbiol. 165, 206–212.

Fiedler, G., Pajatsch, M., Bock, A., 1996. Genetics of novel starch utilisation pathway present in *Klebsiella oxytoca*. J. Mol. Biol. 256, 279–291.

Flourie, B., Molis, C., Achour, L., Dupas, H., Hatat, C., Rambaud, J.C., 1993. Fate of β-cyclodextrin in the human intestine. J. Nutr. 123, 676–680.

Gerloczy, A., Fonagy, A., Keresztes, P., Perlaky, L., Szejtli, J., Arzneim, F., 1985. Absorption, distribution, excretion and metabolism of orally administered ^{14}C-β-cyclodextrin in rat. Drug Res. 35, 1042–1047.

Ghosh, P.B., Whitehouse, M.W., 1968. 7-Chloro-4-nitrobenzo-2-oxa-1,3-diazole: a new fluorogenic reagent for amino acids and other amines. Biochem. J. 108, 155–156.

Grouselle, M., Tueux, O., Dabadie, P., Georgescaud, D., Mazat, J.P., 1990. Effect of local anaesthetics on mitochondrial membrane potential in living cells. Biochem. J. 271, 269–272.

Guldberg, P., Straten, P.T., Brick, A., Ahrenkiel, V., Kirkin, A.F., Zeuthen, J., 1997. Disruption of the MMAC1/PTEN gene by deletion or mutation is a frequent event in malignant melanoma. Cancer Res. 57, 3660–3663.

Hamasaki, K., Ikeda, H., Nakamura, A., Ueno, A., Toda, F., Suzuki, I., Osa, T., 1993. Fluorescent sensors of molecular recognition. Modified cyclodextrins capable of exhibiting guest-responsive twisted intramolecular charge transfer fluorescence. J. Am. Chem. Soc. 115, 5035–5040.

Hanessian, S., 1969. Sugar lactams. 111. Synthesis of five- six-, and seven-membered analogs. J. Org. Chem. 34, 675–681.

Hardegger, E., Zanetti, G., Steiner, K., von krist, P.H., 1963. 6-Desoxy-6-amino-β-glucosehydrochlorid und konstitution einiger zwischenprodukte. Helv. Chim. Acta 26, 282–287.

Higashi, Y., Nakamura, S., Matsumura, H., Fujii, Y., 2006. Simultaneous liquid chromatographic assay of amantadine and its four related compounds in phosphate-buffered saline using 4-fluoro-7-nitro-2,1,3-benzoxadiazole as a fluorescent derivatization reagent. Biomed. Chromatogr., 423–428.

Higuchi, T., Connors, K.A., 1965. In: Reilly, C.N. (Ed.), Advances in Analytical Chemistry Instrumentation, vol. 4. Wiley-Interscience, New York, pp. 117–212.

Hirayama, F., Yamamoto, M., Uekama, K., 1992. Acid-catalyzed hydrolysis of maltosyl-beta-cyclodextrin. J. Pharm. Sci. 81, 913–916.

Hovgaard, L., Bronsted, H., 1995. Drug delivery studies in Caco-2 monolayers. IV. Absorption enhancer effects of cyclodextrins. Pharm. Res. 12, 1328–1332.

Ikeda, H., Murayama, T., Ueno, A., 2006. Bile acids-selective chemosensors based on NBD-amine-modified cyclodextrins. J. Inclusion Phenom. Macrocyclic Chem. 56, 101–105.

Irie, T., Uekama, K., 1997. Pharmaceutical application of cyclodextrin. III. Toxicological issues and safety evaluation. J. Pharm. Sci. 86, 147–162.

Johnson, L.V., Walsh, M.L., Chen, L.B., 1980. Localization of mitochondria in living cells with rhodamine 123. Proc. Natl. Acad. Sci. 77, 990–994.

Kilsdonk, E.P.C., Yancey, P.G., Stoudt, G.W., Bangerter, F.W., Johnson, W.J., Phillips, M.C., Rothblat, G.H., 1995. Cellular cholesterol efflux mediated by cyclodextrins. J. Biol. Chem. 270, 17250–17256.

Knowles, B.B., Howe, C.C., Aden, D.P., 1980. Human hepatocellular carcinoma cell lines secrete the major plasma proteins and hepatitis B surface antigen. Science 209, 497–499.

Kubota, Y., Fukuda, M., Muroguchi, M., Koizumi, K., 1996. Absorption, distribution and excretion of β-cyclodextrin and glucosyl-β-cyclodextrin in rats. Biol. Pharm. Bull. 19, 1068–1072.

Lambert, D., O'Neill, C.A., Padfield, P.J., 1980. Methyl-beta-cyclodextrin increases permeability of Caco-2 cell monolayers by displacing specific claudins from cholesterol rich domains associated with tight junctions. Cell. Physiol. Biochem. 20, 495–506.

Lambert, D., O'Neill, C.A., Padfield, P.J., 2005. Depletion of Caco-2 cell cholesterol disrupts barrier function by altering the detergent solubility and distribution of specific tight-junction proteins. Biochem. J. 387 (Pt 2), 553–560.

Larsen, T., Solberg, S., Johansen, R., Jorgensen, L., 1988. Effect of cooling on the intracellular concentrations of Na^+ K^+ and Cl^- in cultured human endothelial cells. Scand. J. Clin. Lab. Invest. 48, 565–571.

Marttin, E., Verhoef, C.J., Cullander, C., Romeijn, S.G., Nagelkerke, J.F., Merkus, F.W., 1997. Confocal laser scanning microscopic visualization of the transport of dextrans after nasal administration to rats: effects of absorption enhancers. Pharm. Res. 4, 631–637.

Marttin, E., Verhoef, J.C., Spies, F., Van der Meulan, J., Nagelkerke, J.F., Koerten, H.K., Merkus, F.W., 1999. The effect of methylated beta-cyclodextrins on the tight junctions of the rat nasal respiratory epithelium: electron microscopic and confocal laser scanning microscopic visualization studies. J. Control. Rel. 57, 205–213.

Masson, M., Loftsson, T., Masson, G., Stefansson, E., 1999. Cyclodextrins as permeation enhancers: some theoretical evaluations and in vitro testing. J. Control. Rel. 59, 107–118.

Matilainen, L., Toropainen, T., Vihola, H., Hirvonen, J., Järvinen, T., Jarho, P., Järvinen, K., 2008. In vitro toxicity and permeation of cyclodextrins in Calu-3 cells. J. Control. Rel. 126, 10–16.

Matsubara, K., Abe, K., Irie, T., Uekama, K., 1995. Improvement of nasal bioavailability of luteinizing hormone-releasing hormone agonist, buserelin, by cyclodextrin derivatives in rats. J. Pharm. Sci. 84, 1295–1300.

Miller, G.G., Brown, K., Ballangrud, A.M., Barajas, O., Xiao, Z., Tulip, J., Lown, W.J., Leithoff, J.M., Allalunis-Turner, J.M., Mehta, R.D., Moore, R.B., 1997. Preclinical assessment of hypocrellin B and hypocrellin B derivatives as sensitizers for

photodynamic therapy of cancer: progress update. Photochem. Photobiol. 65, 714–722.
Miyazawa, I., Ueda, H., Nagase, H., Endo, T., Kobayashi, S., Nagai, T., 1995. Physicochemical properties and inclusion complex formation of delta-cyclodextrin. Eur. J. Pharm. Sci. 3, 153–162.
Neufeld, E.B., Cooney, A.M., Pitha, J., Dawidowicz, E.A., Dwyer, N.K., Pentchev, P.G., Blanchette-Mackie, E.J., 1996. Intracellular trafficking of cholesterol monitored with a cyclodextrin. J. Biol. Chem. 271, 21604–21613.
Ostlund, R.E., Seemayer Jr., R., Gupta, S., Kimmel, R., Ostlund, E.L., Sherman, W.R., 1996. A stereospecific myo-inositol/D-chiro-inositol transporter in HepG2 liver cells. J. Biol. Chem. 271, 10073–10078.
Pajatsch, M., Gerhart, M., Peist, R., Horlacher, R., Boos, W., Bock, A., 1998. The periplasmic cyclodextrin binding protein CymE from *Klebsiella oxytoca* and its role in maltodextrin and cyclodextrin transport. J. Bacteriol. 180, 2630–2635.
Petter, R.C., Salek, J.S., Sikorski, C.T., Kumaravel, G., Lin, F.T., 1990. Cooperative binding by aggregated mono-6-(alkylamino)-β-cyclodextrins. J. Am. Chem. Soc. 112, 3860–3868.
Rodal, S.K., Skretting, G., Garred, O., Vilhardt, F., van Deurs, B., Sandvig, K., 1999. Extraction of cholesterol with methyl-beta-cyclodextrin perturbs formation of clathrin-coated endocytic vesicles. Mol. Biol. Cell. 10, 961–974.
Skoog, D.A., Holler, F.J., Nieman, T.A., 1998. Principles of Instrumental Analysis, fifth ed. Harcourt Brace & Company Press, Orlando, FL.
Speizer, L., Haugland, R., Kutchai, H., 1985. Asymmetric transport of a fluorescent glucose analogue by human erythrocytes. Biochim. Biophys. Acta 815, 75–84.
Szejtli, J., Gerloczy, A., Fonagy, A., 1980. Intestinal absorption of ^{14}C-labelled β-cyclodextrin in rats. Arzneim - Forsch 30, 808–810.
Szejtli, J., 1988. In: Davies, J.E.D. (Ed.), Cyclodextrin Technology. Kluwer Academic Press, Dordrecht, The Netherlands.
Tekeo, K., Mitoh, H., Uemura, K., 1989. Selective chemical modification of cyclomalto-oligosaccharides via tert-butyldimethylsilylation. Carbohydr. Res. 187, 203–221.
Yang, X.-H., Singh, S., Kumar, P., Diakur, J., Wiebe, L.I., 2009. β-Cyclodextrin complexes of hydrolyzable adamantanoyl-IUdR prodrugs-radioiodination and biodistribution in mice bearing implanted KBALB tumor. Curr. Radiopharmaceut. 2, 137–142.